

Efficient Gene Suppression by DNA/DNA Double-Stranded Oligonucleotide *In Vivo*

Yutaro Asami,^{1,2,4} Tetsuya Nagata,^{1,2,4} Kotaro Yoshioka,^{1,2,4} Taiki Kunieda,^{1,2} Kie Yoshida-Tanaka,^{1,2} C. Frank Bennett,³ Punit P. Seth,³ and Takanori Yokota^{1,2}

¹Department of Neurology and Neurological Science, Graduate School of Medical and Dental Sciences, Tokyo Medical and Dental University (TMDU), Tokyo, Japan;

²Center for Brain Integration Research, Tokyo Medical and Dental University (TMDU), Tokyo, Japan; ³Ionis Pharmaceuticals, Carlsbad, CA, USA

We recently reported the antisense properties of a DNA/RNA heteroduplex oligonucleotide consisting of a phosphorothioate DNA-gapmer antisense oligonucleotide (ASO) strand and its complementary phosphodiester RNA/phosphorothioate 2'-O-methyl RNA strand. When α -tocopherol was conjugated with the complementary strand, the heteroduplex oligonucleotide silenced the target RNA more efficiently *in vivo* than did the parent single-stranded ASO. In this study, we designed a new type of the heteroduplex oligonucleotide, in which the RNA portion of the complementary strand was replaced with phosphodiester DNA, yielding an ASO/DNA double-stranded structure. The ASO/DNA heteroduplex oligonucleotide showed similar activity and liver accumulation as did the original ASO/RNA design. Structure-activity relationship studies of the complementary DNA showed that optimal increases in the potency and the accumulation were seen when the flanks of the phosphodiester DNA complement were protected using 2'-O-methyl RNA and phosphorothioate modifications. Furthermore, evaluation of the degradation kinetics of the complementary strands revealed that the DNA-complementary strand as well as the RNA strand were completely cleaved *in vivo*. Our results expand the repertoire of chemical modifications that can be used with the heteroduplex oligonucleotide technology, providing greater design flexibility for future therapeutic applications.

INTRODUCTION

Nucleic acid-based therapeutics represent a promising technology platform to manipulate gene targets that are otherwise difficult to modulate by conventional low-molecular-weight compounds and antibodies.¹ Antisense oligonucleotides (ASOs) bind to their complementary RNA (coRNA) by Watson-Crick base pairing in cells and regulate RNA functions to produce pharmacological effects. Gapmer ASOs have a central gap region of phosphorothioate (PS)-modified DNA flanked on either end by chemical modifications, such as locked nucleic acid (LNA)/bridged nucleic acid (BNA), 2'-O-methoxy-ethyl (MOE), and 2',4'-constrained 2'-O-ethyl bridged nucleic acid (cEt). These modifications increase resistance against nucleases and enhance the affinity for target RNA.² Gapmer ASOs bind to their target RNA in cells, and the resulting duplex is a substrate for RNase H1, a ubiquitously expressed endonuclease³ that selectively cleaves the RNA strand of the heteroduplex, suppressing expression of the corresponding gene.⁴ Mul-

tiples ASOs have been recently approved for clinical application by the US Food and Drug Administration and other regulatory agencies (e.g., mipomersen,⁵ eteplirsen,⁶ nusinersen,⁷⁻⁹ and inotersen^{10,11}). More than 40 ASOs are currently being investigated in clinical trials for treatment of a variety of disease indications.¹²

We have previously developed a heteroduplex oligonucleotide (HDO) in which the single-stranded ASO was hybridized to coRNA that was further conjugated with α -tocopherol (Toc). The Toc-HDO (coRNA) design significantly enhanced the antisense potency of the parent ASO in mouse liver.¹³⁻¹⁷ We also showed that the coRNA of the Toc-HDO (coRNA) is stable in the serum and that conjugation with Toc enhances productive delivery to the liver by enhancing association with serum lipoproteins. Toc-HDO (coRNA) was taken up into cells mostly in the intact form, after which the coRNA strand was cleaved by RNase H with the release of the parent ASO inside the cells. Cellular uptake of Toc-HDO (coRNA) was initiated within ~10 min. Therefore, we hypothesized that the complementary strand does not necessarily need to be phosphodiester (PO) RNA and can be replaced with PO DNA. DNA potentially has some advantages over RNA, as it is chemically more stable and less expensive to manufacture than RNA. Hence, we replaced the complementary PO RNA strand in the HDO with PO DNA, creating a DNA/DNA double-stranded molecule, named HDO (coDNA). Although double-stranded DNA (dsDNA) is not a substrate for RNase H, it can be degraded intracellularly by endonucleases belonging to the DNase I and II families.¹⁸ DNase I is expressed primarily in the exocrine cells of the digestive tract and is also present in the serum, where its expression level is approximately 15-fold lower than in the liver.¹⁹ DNase II is expressed in lysosomes throughout the body; however, it is not present in the serum.²⁰ This dsDNA structure may therefore be stable in

Received 30 August 2020; accepted 19 October 2020;

<https://doi.org/10.1016/j.ymthe.2020.10.017>.

⁴These authors contributed equally to this work.

Correspondence: Takanori Yokota, Department of Neurology and Neurological Science, Graduate School of Medical and Dental Sciences, Tokyo Medical and Dental University (TMDU), 1-5-45 Yushima, Bunkyo-ku, Tokyo 113- 8519.

E-mail: tak-yokota.nuro@tmd.ac.jp

Correspondence: Punit P. Seth, Ionis Pharmaceuticals, 2855 Gazelle Court, Carlsbad, CA 92010, USA.

E-mail: pseth@ionisph.com

the blood, and the coDNA strand can be degraded intracellularly by DNases or related nucleases.

In this study, we investigated the effects of Toc-HDO (coDNA) molecules on mRNA expression levels of three gene targets by using parent ASOs of different structures and lengths. We also examined coDNA strand structure-activity relationships of Toc-HDO (coDNA) molecules and evaluated degradation kinetics of the Toc-HDO (coDNA) complementary strand over time in mouse liver.

RESULTS

Toc-HDO (coDNA) Suppresses *Apob* mRNA More Efficiently Than the 13-mer Parent ASO

We have previously designed a Toc-HDO (coRNA) that consists of a DNA/LNA gapmer ASO targeting apolipoprotein B (*Apob*) mRNA and a coRNA strand.¹³ As described previously, the coRNA strand had 8–10 PO RNAs flanked by two or three 2'-*O*-methyl RNAs (2'OMes)^{21,22} with PS modifications²³ to enhance stability against exonuclease digestion in the blood and endosomal compartments. Toc was conjugated to the 5' end of the coRNA to enhance interaction with plasma lipoproteins and facilitate distribution and cellular uptake. In the present study, we designed a Toc-HDO (coDNA), in which the central fragment was replaced by PO DNA, as well as a single-stranded Toc-ASO with Toc directly conjugated to its 5' end with a stable PS linker (Figure 1A).

To evaluate the *in vivo* potency of these two types of Toc-HDOs, we measured expression levels of *Apob* mRNA in mouse liver 1 day after intravenous (i.v.) injection of the single-stranded parent ASO or Toc-HDOs (Figure 1B). Toc-HDO (coRNA) showed a higher knockdown efficacy than did the single-stranded ASO, as has been previously reported.¹³ Toc-HDO (coDNA) also showed high knockdown effects similar to those of Toc-HDO (coRNA). However, Toc-ASO, HDO (coRNA), and HDO (coDNA) did not increase the knockdown efficacy compared to that achieved by the parent ASO. The relative ASO strand concentrations in the liver after injection of Toc-HDO (coDNA) and Toc-HDO (coRNA) were similar (Figure 1C). The high knockdown effect of Toc-HDO (coDNA) was also seen 7 days after injection (Figures 1D and S1). The suppressive effect of Toc-HDO (coDNA) at a dose of 107.7 nmol/kg on *Apob* mRNA level was comparable to that conferred by Toc-HDO (coRNA) at a dose of 79.4 nmol/kg and by the single-stranded ASO at a dose of 693.6 nmol/kg (Figure S2). To evaluate the phenotypic effect of silencing *Apob* mRNA, we assessed low-density lipoprotein (LDL) cholesterol levels in the serum. Both Toc-HDO (coDNA) and Toc-HDO (coRNA) significantly reduced LDL cholesterol compared to the single-stranded ASO after i.v. (Figures 1E and S3) or subcutaneous injections (Figure S4).

Toc-HDO (coDNA) Suppresses *Malat1* RNA More Efficiently Than the 16-mer Parent ASO

Next, the effect of the 16-mer ASO targeting metastasis-associated lung adenocarcinoma transcript-1 (*Malat1*) RNA was compared to that of the respective Toc-HDOs (coRNA and coDNA). The effects

of Toc-ASO, HDO (coRNA), and HDO (coDNA) were also examined (Figure 2A). Both Toc-HDO (coRNA) and Toc-HDO (coDNA) maintained their double-stranded structure after a 6-h incubation in mouse serum (Figure S5). Three days after i.v. injection, both Toc-HDO (coRNA) and Toc-HDO (coDNA) suppressed target RNA more efficiently than did the parent ASO (Figure 2B). Toc-ASO did not have a higher suppressive effect than the parent ASO.²⁴ Furthermore, at 3 days after i.v. administration, the *Malat1* RNA level significantly decreased in a dose-dependent manner in the Toc-HDO (coRNA) and Toc-HDO (coDNA) groups (Figure 2C). The doses that had the half-maximal effect (ED₅₀) were 272.4 nmol/kg for ASO, 138.0 nmol/kg for Toc-HDO (coRNA), and 166.3 nmol/kg for Toc-HDO (coDNA). There were also no significant differences in the liver accumulations of ASO after injections of Toc-HDO (coRNA) and Toc-HDO (coDNA) (Figure 2D).

Toc-HDO (coDNA) with cEt ASO Potently Suppresses Gene Expression

The cEt modification confers a comparable enhancement in RNA affinity; however, it improves nuclease stability and safety as compared with that achieved with LNA,²⁵ and more than 10 cEt ASOs are currently in clinical development. To determine whether ASO chemistry in Toc-HDO influences potency, we examined a 14-mer ASO that targeted mouse scavenger receptor class B member 1 (*Scarb1*), in which the cEt wing replaced that of LNA as previously described.²⁶ In the present study, we evaluated the same designs of Toc-HDO (coRNA) and Toc-HDO (coDNA) hybridized to ASO with the cEt wing. In addition, we evaluated Toc-HDO with a complementary strand fully modified with 2'-fluoro RNA (2'F), a commonly used RNA modification to enhance nuclease stability, designated as Toc-HDO (full 2'F) (Figure 3A). We determined the extent of *Scarb1* mRNA knockdown in mouse liver 3 days after i.v. injections of these Toc-HDOs. As in the case with the two sequences described above, Toc-HDO (coRNA) and Toc-HDO (coDNA) suppressed *Scarb1* mRNA more efficiently than did the parent ASO. There were no significant differences in the inhibitory effect between the two designs (Figure 3B). Serum aspartate aminotransferase (AST), alanine aminotransferase (ALT), and blood urea nitrogen (BUN) levels were not significantly altered compared with those in untreated mice (Table 1). Somewhat surprisingly, the inhibitory effect on the *Scarb1* mRNA level was almost entirely attenuated in the case of Toc-HDO (full 2'F) at the dose of 234.1 nmol/kg (Figure 3B). When the dose was increased, silencing was observed following administration of Toc-HDO (full 2'F). However, an approximately 10-fold dose was required to produce similar silencing with other Toc-HDOs (Figures 3B and S6). To further investigate whether this significant decrease in activity with the 2'F complementary strand could be replicated in cells, all HDO constructs were evaluated in primary hepatocytes. Similar potency for *Scarb1* mRNA knockdown was observed for Toc-HDO (coRNA) and Toc-HDO (coDNA) (Figures 3C and 3D). The HDO without conjugated Toc also showed similar potency, suggesting that Toc conjugation does not change the intrinsic potency of the HDO, but rather likely enhances distribution to tissues in mice relative to that achieved with the single-stranded ASO. Toc-HDO

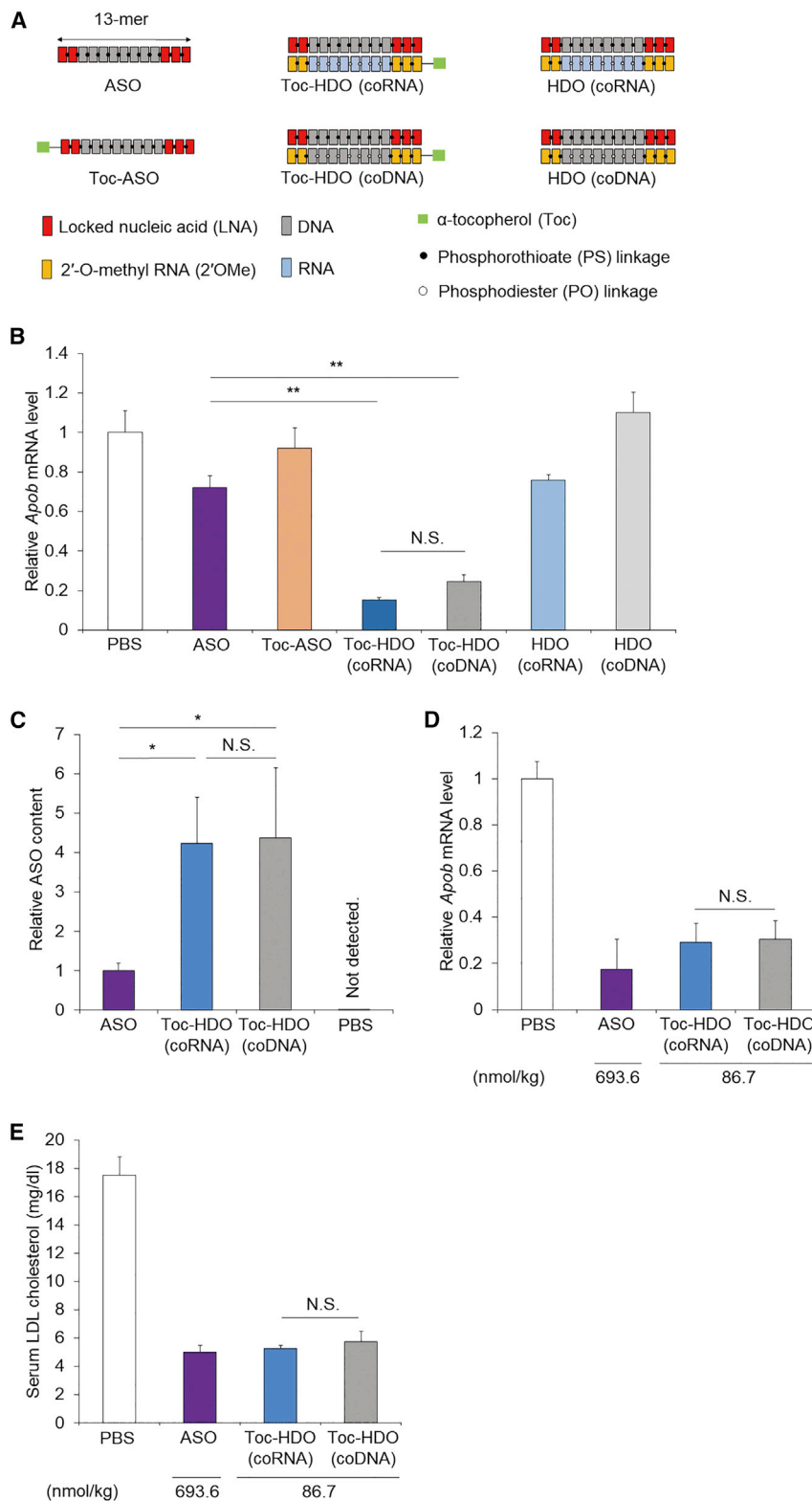


Figure 1. Enhanced *In Vivo* Inhibitory Effects of Toc-HDO (coDNA) on the *Apob* mRNA Expression and LDL Cholesterol Levels

(A) Structures of the parent 13-mer ASO, Toc-ASO, Toc-HDO (coRNA), Toc-HDO (coDNA), HDO (coRNA), and HDO (coDNA) targeting mouse *Apob* mRNA. (B) Quantitative real-time PCR analysis of the relative *Apob* mRNA expression levels in mouse liver 1 day after intravenous injection of the parent ASO, Toc-ASO, Toc-HDO (coRNA), Toc-HDO (coDNA), HDO (coRNA), or HDO (coDNA) at a dose of 86.7 nmol/kg as the parent ASO. (C) Quantitative real-time PCR analysis of the relative parent ASO content in mouse liver after intravenous injection of ASO and Toc-HDOs at a dose of 86.7 nmol/kg. (D) Quantitative real-time PCR analysis of the relative parent ASO mRNA expression levels in mouse liver and (E) serum LDL cholesterol levels 7 days after intravenous injection of the parent ASO at a dose of 693.6 nmol/kg, with Toc-HDO (coRNA) or Toc-HDO (coDNA) at a dose of 86.7 nmol/kg. Data are presented as the mean \pm standard error of the mean; $n = 3$ or 4 per group; * $p < 0.05$, ** $p < 0.01$. N.S., not significant.

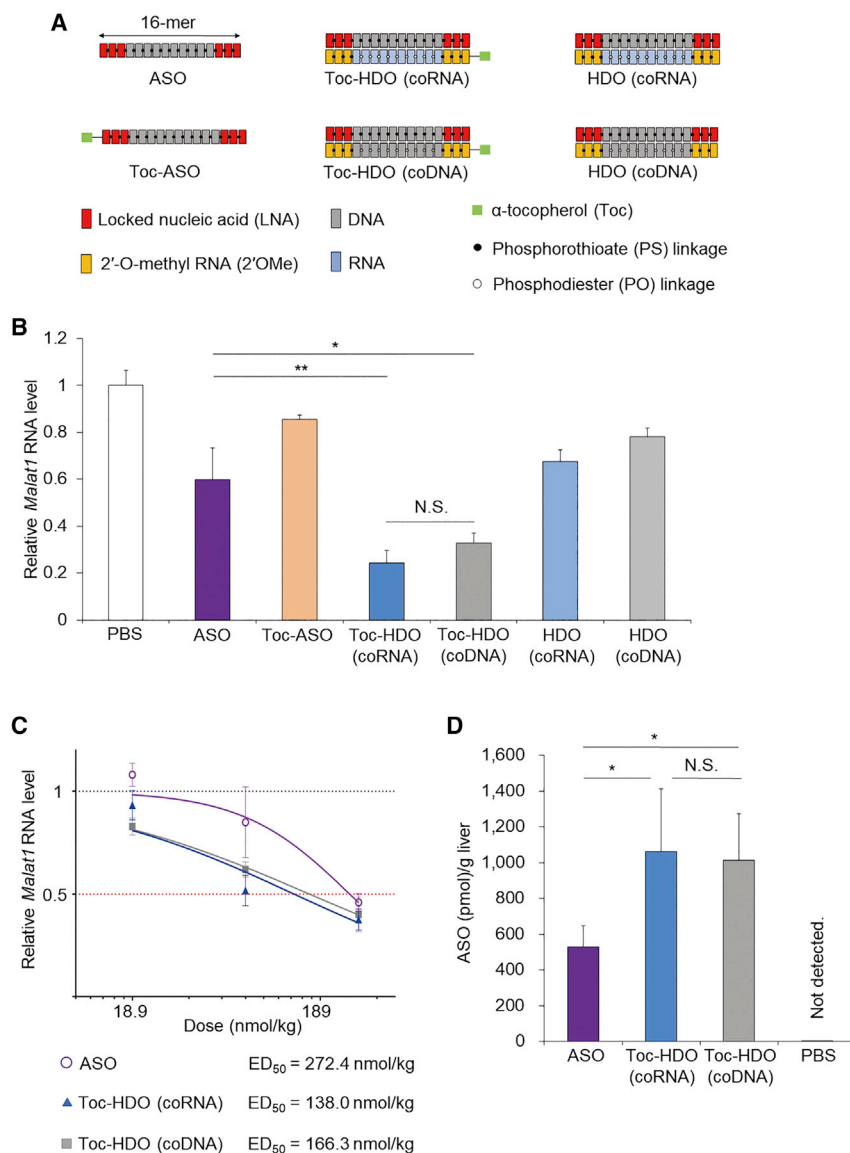


Figure 2. Enhanced *In Vivo* Inhibitory Effect of Toc-HDO (coDNA) on Expression of *Malat1* RNA

(A) Structures of the parent 16-mer ASO and Toc-ASO, Toc-HDO (coRNA), Toc-HDO (coDNA), HDO (coRNA), and HDO (coDNA) targeting mouse *Malat1* RNA. (B) Quantitative real-time PCR analysis of the relative *Malat1* RNA expression levels in mouse liver 3 days after intravenous injection of the parent ASO, Toc-ASO, Toc-HDO (coRNA), Toc-HDO (coDNA), HDO (coRNA), or HDO (coDNA) at a dose of 151.2 nmol/kg as the parent ASO. (C) Dose-response relationship of *Malat1* RNA level inhibition in mouse liver 3 days after injection of the parent ASO, Toc-HDO (coRNA), or Toc-HDO (coDNA). (D) Quantitative real-time PCR analysis of ASO amount in mouse liver 3 days after injection of the parent ASO, Toc-HDO (coRNA), or Toc-HDO (coDNA). Data are presented as the mean \pm standard error of the mean; $n = 3$ or 4 per group; * $p < 0.05$, ** $p < 0.01$. N.S., not significant.

PO were introduced at both ends of the coDNA targeting *Malat1* RNA (Figure 4D). When evaluated 3 days after i.v. injection in mice, Toc-HDO (coDNA) (six 2'OMes, six PSs) had the strongest inhibitory effect (Figure 4E), indicating that both 2'OMe and PS at both ends of the complementary strand effectively maintained Toc-HDO (coDNA) potency.

Next, to investigate whether Toc-HDOs using long ASOs can improve RNA silencing, we evaluated *in vivo* potency of Toc-HDOs using a 20-mer DNA/MOE gapmer targeting *Malat1* RNA (Figure S7A). Both Toc-HDO (coRNA) and Toc-HDO (coDNA) comprising this ASO similarly improved RNA silencing (Figure S7B).

Toc-HDO (coDNA) Complementary Strand Degrades within 6 h in Mouse Liver

In our previous report, we showed that coRNA was cleaved in the liver to release the parent ASO from Toc-HDO.¹³ To determine the fate of the DNA complement, northern blot analysis for detecting the complementary strand was performed. To facilitate detection of the complementary strand, a single-stranded 20-mer PO 2'OMe was introduced on the 3' end of the coRNA and coDNA to hybridize the northern blot probe (Figure 5A). These Toc-HDOs with extended 2'OMe were administered by i.v. injections, and the mice were sacrificed after 6 h, 1 day, and 3 days. The livers were harvested, and the extracted RNAs were evaluated by northern blot. Following Toc-HDO (coRNA) injection, the full-length complementary strands were observed 6 h after administration, and small amounts were still detected at day 1; however, they disappeared entirely by day 3 (Figure 5B), with concomitant increases in fragments comprising the fully modified 2'OMe tail. In contrast, none of the full-length complementary strands was observed in the Northern blot

(full 2'F) had an approximately 2- to 3-fold lower inhibitory effect compared to that of other molecules.

Structure-Activity Relationships of Toc-HDO (coDNA)

Next, we optimized the number of 2'OMe and PS modifications on the coDNA. First, coDNAs with 0, 2, or 5 PSs without any 2'OMes at both ends were prepared for the 13-mer ASO targeting *Apob* mRNA (Figure 4A). The structures with PS were more effective than those without PS in suppressing *Apob* mRNA expression in mouse liver (Figure 4B). Furthermore, the Cy5-labeled parent ASO of the Toc-HDO (coDNA)s were injected into mice i.v., and liver fluorescence intensity was measured at 6 h after injection. The amount of the Toc-HDO (coDNA) ASO strand in the liver was significantly higher for the structure with five PS moieties (Figure 4C). Next, 2'OMe or DNA and PS or

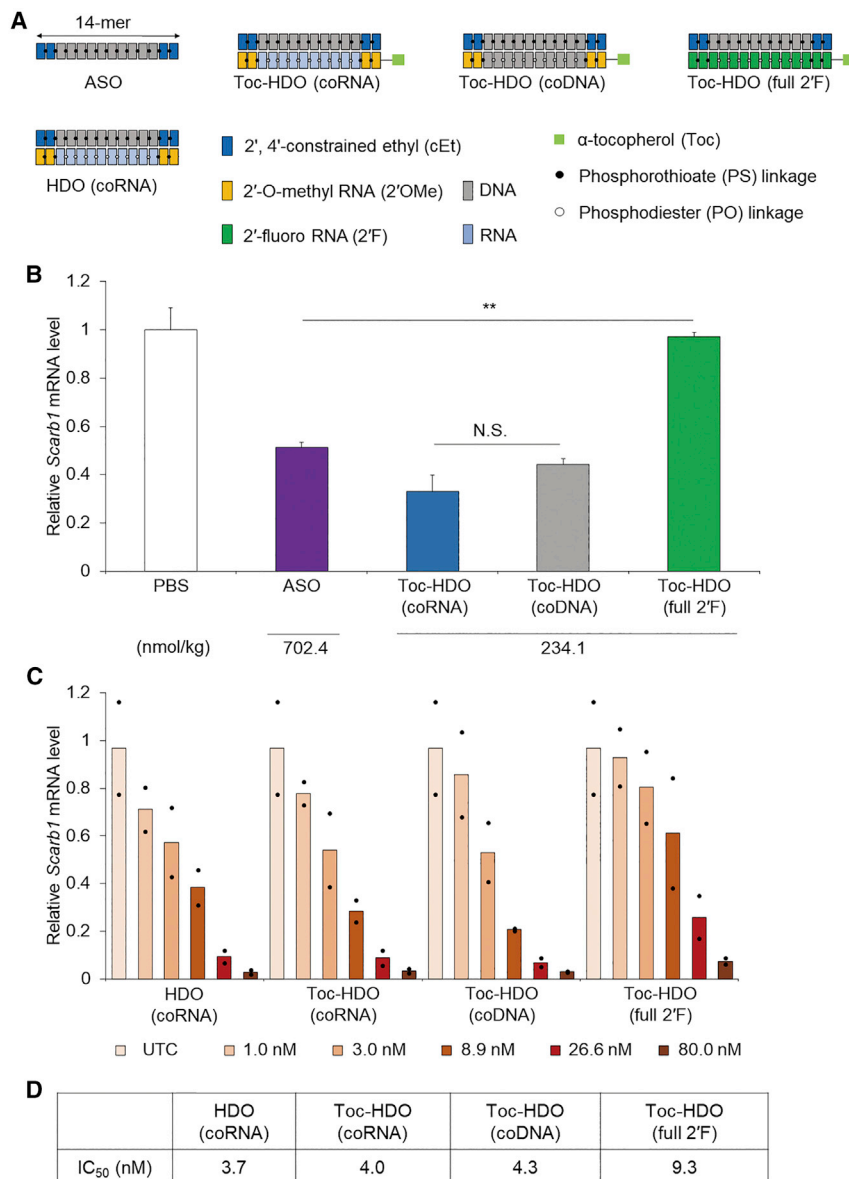


Figure 3. Enhanced *In Vivo* Inhibitory Effect of Toc-HDO (coDNA) on *Scarb1* mRNA Expression Level

(A) Design of ASO with cEt and HDO (coRNA), Toc-HDO (coRNA), Toc-HDO (coDNA), and Toc-HDO (full 2'F) targeting mouse *Scarb1* mRNA. (B) Quantitative real-time PCR analysis of relative mouse *Scarb1* mRNA expression in livers from mice 3 days after single intravenous injections of 702.4 nmol/kg for ASO or 234.1 nmol/kg for Toc-HDOs as the parent ASO. Data are presented as the mean \pm standard error of the mean; $n = 3$ or 4 per group; ** $p < 0.01$. N.S., not significant. (C) Primary mouse hepatocytes isolated from male BALB/c mice were treated with double-stranded oligonucleotides by free uptake. Quantitative real-time PCR analysis of relative mouse *Scarb1* mRNA expression was performed. Data are the average of two independent experiments. The value of each result is displayed as a dot. (D) 50% inhibitory concentration (IC₅₀) in the experiment (C).

ASO activity. Moreover, the amount of Toc-HDO (coDNA) that reached the liver 6 h after administration was less than that of Toc-HDO (coRNA), although it had achieved the same level after 3 days (Figures S8 and 2D).

DISCUSSION

We have recently described an HDO (coRNA) molecule in which an RNase H1 active gapper ASO is duplexed using a coRNA strand conjugated with Toc. This Toc-HDO (coRNA) design significantly enhanced the parent ASO potency not only in the liver¹³ but also in the endothelial cells of the blood-brain barrier.¹⁶ In addition, the HDO (coRNA) technology improved the efficacy of microRNA-targeted therapeutic oligonucleotides.¹⁷

Single-stranded PS ASOs interact with plasma and cell-surface proteins, which facilitates ASO delivery to peripheral tissues.²⁷ PS ASOs associate primarily with albumin in plasma; however, they can also

interact with proteins such as histidine-rich glycoprotein³ and α 2-macroglobulin.²⁸ The latter interactions can reduce ASO potency, as ASOs can be shuttled into non-productive tissue compartments. Furthermore, PS ASOs have been shown to interact with the Stabilin class of scavenger receptors,^{29,30} epidermal growth factor receptors,^{31,32} and asialoglycoprotein receptors.³³ These interactions promote uptake of ASOs into the endothelial and other cells of the liver. PS ASO preferentially accumulates in non-parenchymal cells of the liver, which may limit its efficacy toward genes expressed in hepatocytes. In contrast, the double-stranded design in the HDO can mitigate some of the undesirable protein-binding properties of PS ASOs.³⁴ Moreover, conjugation with Toc enhances ASO association with plasma lipoproteins and promotes its uptake by lipoprotein receptors, leading to improved ASO accumulation and potency in the parenchymal cells of the liver.¹³

already in 6 h after the administration of Toc-HDO (coDNA) (Figure 5B). Therefore, we performed a follow-up experiment for Toc-HDO (coDNA) in which mice were sacrificed 10 min and 1 h after injection. The full-length complementary strand was observed at these two time points (Figure 5C). These results showed that the complementary strand of Toc-HDO (coDNA) degraded faster than did that of Toc-HDO (coRNA). To determine whether Toc-HDO (coDNA) has an earlier onset of action than Toc-HDO (coRNA), mice were injected i.v. with 75.6 nmol/kg Toc-HDO (coRNA), 75.6 nmol/kg Toc-HDO (coDNA), or 226.8 nmol/kg ASO targeting *Malat1* RNA, and the livers were collected at 6, 12, or 18 h after injection. The suppressive effects on *Malat1* levels were similar at all of these time points (Figure 5D). This observation suggests that the speed of the complementary strand degradation of HDO did not affect the onset of intrinsic

Table 1. Serum AST, ALT, and BUN Levels at 3 Days after an Intravenous Injection of PBS, Parent ASO, or HDOs Targeting *Scarb1* mRNA

	Dose (nmol/kg)	AST (U/L)	ALT (U/L)	BUN (mg/dL)
PBS		72.3 ± 4.6	36.3 ± 6.4	32.7 ± 0.8
ASO	702.4	57.5 ± 4.0	30.5 ± 5.4	30.1 ± 1.6
Toc-HDO (coRNA)	234.1	53.7 ± 4.9	24.3 ± 0.7	31.0 ± 1.7
Toc-HDO (coDNA)	234.1	67.7 ± 8.8	28.7 ± 1.9	34.0 ± 0.4
Toc-HDO (full 2'F)	234.1	89.8 ± 11.9	27.3 ± 0.5	31.8 ± 2.0

Data are presented as the mean ± standard error of the mean; n = 3 or 4 per group. ALT, alanine aminotransferase; AST, aspartate aminotransferase; BUN, blood urea nitrogen; PBS, phosphate-buffered saline.

In our initial HDO (coRNA) design, the complementary PO RNA strand was paired with the DNA gap region of the ASO, whereas the flanking nucleotides were protected against exonuclease digestion with PS and 2'OMe modifications. This design is stable in the blood; however, it is susceptible to RNase H-mediated degradation in the cytoplasm that would release the parent ASO.¹³ Once released, the parent ASO is free to hybridize to its coRNA target and suppress gene expression by RNase H1-mediated degradation of the targeted RNA.

Considering that dsDNA is generally more stable than RNA, we expected substantial delivery of the DNA/DNA duplex of HDO (coDNA) to the liver before its degradation in the serum. Indeed, a certain amount of Toc-HDO (coDNA) was taken up by the liver within 10 min after i.v. injection, and most of the dsDNA was not degraded in the serum for more than 6 h. Therefore, we investigated the Toc-HDO (coDNA), in which the PO RNA region of the complementary strand from the original design was completely replaced by PO DNA. We found that Toc-HDO (coDNA) showed similar overall liver accumulation and nearly identical potency for reducing targeted RNA expression in the liver to those of Toc-HDO (coRNA). Given that HDO (coDNA) is not degraded by RNase H1, we postulated that this duplex would be recognized by intracellular DNases that would degrade the PO DNA complement to release the DNase-resistant ASO by PS modification. However, at present, it is unclear which fractions of the total HDO (coDNA) were cleaved within the endosomal compartment versus the cytoplasm or the nucleus.

To determine whether there were any differences in the kinetics of degradation for the RNA and DNA complements after cellular uptake, we evaluated both designs by northern blot analysis in time course experiments, by using complementary strands with extended 2'OMe overhangs. We found that a fraction of the full-length RNA (but not DNA) complement could still be detected after 6 h in mouse liver. The follow-up experiments showed that full-length DNA complement was detectable at the 10-min and 1-h time points. Thus, our results suggest that the DNA/DNA duplex is delivered to the liver as a double-stranded structure and then gets degraded more rapidly than the DNA/RNA heteroduplex. One possible explanation is that the DNA/DNA duplex and DNA/RNA heteroduplex are digested in different

intracellular compartments by DNases^{20,35,36} and RNases,³⁷ respectively. Moreover, despite the rapid degradation of Toc-HDO (coDNA), the initiation timing of RNA suppression did not differ from that of Toc-HDO (coRNA). This might be due to multiple factors such as differences in delivery to the liver and intracellular trafficking.

Interestingly, the presence of a fully modified 2'F-complementary strand significantly reduced ASO activity in mice, suggesting that interfering with cleavage of the complementary strand by intracellular nucleases reduces the silencing effect *in vivo*, as 2'F has higher nuclease resistance.³⁸ An alternative possibility is that 2'F-modified nucleic acids are more hydrophobic and interact differently with plasma proteins,³⁹ resulting in the delivery of ASO to non-productive tissue compartments such as lysosomes.

In addition, the complementary strand degradation products may activate innate immune responses. For example, Toll-like receptor (TLR)7/TLR8 recognize single-stranded RNA, which is rich in U and G,^{35,40} while TLR9 recognizes DNA for unmethylated CpG sequences and induces an immune response.⁴¹ These are important variables to consider when selecting DNA or RNA complementary strands, and they thus require further investigations.

In summary, our experiments indicate that the preserved stability of HDO in the serum until uptake by the cells as well as efficient degradation and unwinding of the complementary strand from the ASO strand inside the cells are essential beneficial features of the HDO technology. In addition, PO RNA is dispensable as the complementary strand of HDO and can be replaced by PO DNA. The latter is less expensive and chemically more stable during synthesis than PO RNA. Our findings therefore expand possibilities of the future HDO design and the range of applications of this molecular technology.

MATERIALS AND METHODS

ASOs

A series of DNA/LNA gapmers, coRNAs, and coDNAs designed to target mouse *Apob* mRNA (GenBank: NM_009693), mouse *Malat1* RNA (GenBank: NR_002847.3), or mouse *Scarb1* mRNA (GenBank: NM_016741) were synthesized by Gene Design (Osaka, Japan) and Ionis Pharmaceuticals (Carlsbad, CA, USA). The sequences of ASOs, coRNAs, and coDNAs used in this study are listed in [Supplemental Materials and Methods](#).

Mouse Experiments

For all the mouse experiments, with the exception of that presented in [Figure 3B](#), 4- to 5-week-old wild-type female Crlj:CD1 (ICR) mice were obtained from Oriental Yeast (Tokyo, Japan). ASOs were administered to mice (n = 3–4 per group) according to body weights via tail vein injections. All oligonucleotides were formulated in phosphate-buffered saline (PBS), which was also used as the vehicle. Prior to postmortem analyses, mice were anesthetized with an intraperitoneal injection of 60 mg/kg pentobarbital and then euthanized by a transcardial perfusion with PBS. Blood was collected from the tail vein before perfusion

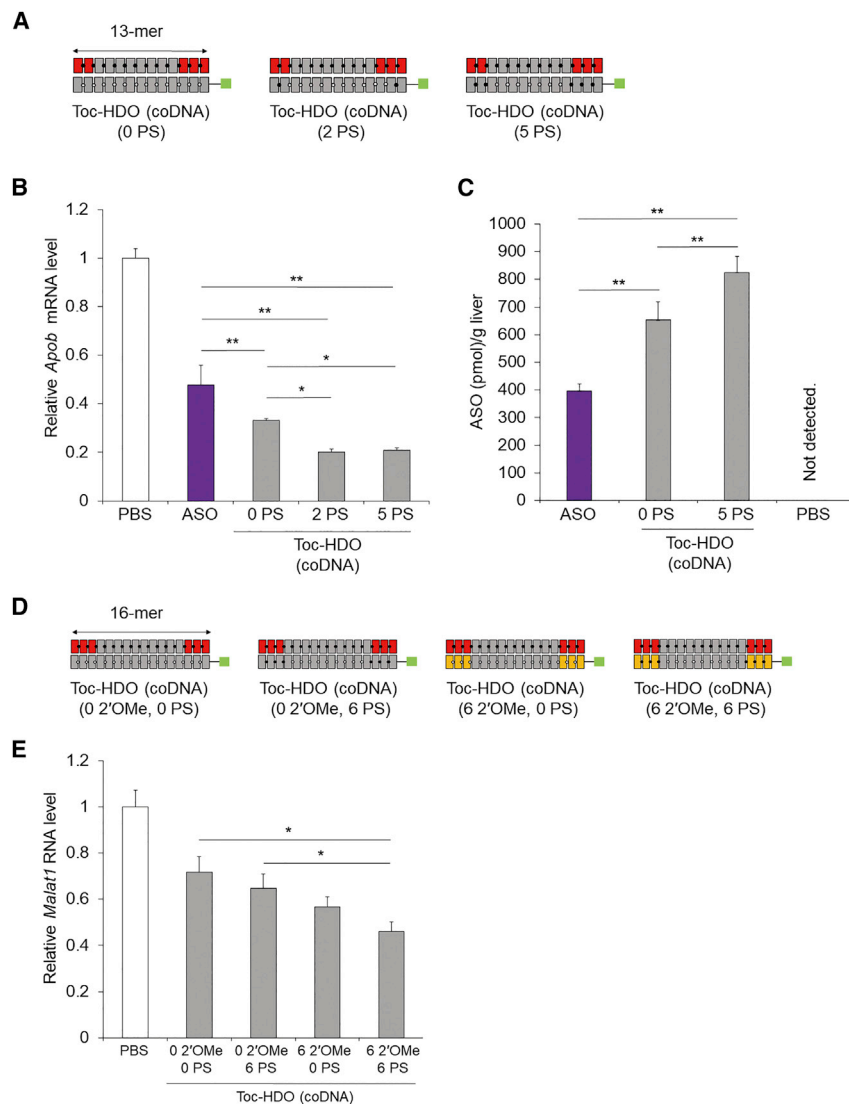


Figure 4. Structure-Activity Relationships of Toc-HDO (coDNA)

(A) Structure of 13-mer Toc-HDO (coDNA) molecules targeting mouse *Apob* mRNA that incorporated no, two, or five PS linkages. (B) Quantitative real-time PCR analysis of the relative *Apob* mRNA expression level in mouse liver 3 days after intravenous injection of the parent ASO and either no PS, two PS, or five PS Toc-HDO (coDNA) at a dose of 173.4 nmol/kg as the parent ASO. (C) Concentrations of Cy5-labeled parent ASO in mouse liver 6 h after intravenous injections of the parent ASO, or no PS and five PS Toc-HDO (coDNA) at a dose of 173.4 nmol/kg. (D) Structures of Toc-HDO (coDNA) (no 2'OMe, no PS), Toc-HDO (coDNA) (no 2'OMe, six PS), Toc-HDO (coDNA) (six 2'OMe, no PS), and Toc-HDO (coDNA) (six 2'OMe, six PS) targeting mouse *Malat1* RNA. (E) Quantitative real-time PCR analysis of the relative *Malat1* RNA expression levels in mouse liver 3 days after intravenous injection of Toc-HDOs illustrated in (D) at a dose of 75.6 nmol/kg. Data are presented as the mean \pm standard error of the mean; n = 4 per group; *p < 0.05, **p < 0.01.

remove impurities and debris. These cells were cultured in plating medium (Williams' medium E and hepatocyte plating supplement pack [Thermo Fisher Scientific, Waltham, MA, USA]) in a humidified incubator at 37°C in a 95% air and 5% CO₂ atmosphere. These primary mouse hepatocytes were plated at a density of 15,000 cells per well into 96-well plates. One day after plating, the cells were exposed to the HDO (coRNA), Toc-HDO (coRNA), Toc-HDO (coDNA), or Toc-HDO (full 2'F) by free uptake and lysed 24 h after treatment.⁴³

Quantitative Real-Time PCR Assay

Total RNA was extracted from mouse liver using Isogen II (Nippon Gene, Tokyo, Japan). For primary hepatocytes, RNA was extracted and purified using RNeasy 96-well plates (QIAGEN, Venlo, the Netherlands). To detect mRNA, RNA was reverse transcribed with PrimeScript reverse transcriptase (Takara Bio, Kusatsu, Japan). The sequences of the primer and probe sets for mouse *Apob*, *Malat1*, and *Actb* (β -actin) genes were as follows: *Apob*, forward, 5'-CACGTGGGCTCCAGCATT-3', reverse, 5'-TCACCAGTCATTTCTGCCTTTG-3', probe, 5'-FAM-CCAATG GTCGGGCACTGCTCAA-TAMRA-3'; *Malat1*, forward, 5'-TGG GTTAGAGAAGGCGTGTACTG-3', reverse, 5'-TCAGCGGCAAC TGGGAAA-3', probe, 5'-FAM-TGTTGGCAGCACCTTCAGG GACT-TAMRA-3'; *Actb*, forward, 5'-CGCGAGCACAGCTTCTT TG-3', reverse, 5'-CATGCCGAGCCGTTGTG-3', probe, 5'-FAM-C ACACCCGCCACCAGTTCGCCATG-TAMRA-3'.

Quantitative real-time PCR analyses were performed using TaqMan primers (Applied Biosystems, Foster City, CA, USA) in a LightCycler 480 system with a LightCycler 480 probes master kit (Roche

to measure the serum level of LDL cholesterol. All protocols were executed in accordance with the ethics and safety guidelines for animal experimentation and were approved by the Ethics Committee of Tokyo Medical and Dental University (#A2019-131C).

In *Scarb1* mRNA target experiments illustrated in Figure 3B, which were conducted at Ionis Pharmaceuticals, C57BL/6J mice aged 8 weeks were obtained from Jackson Laboratory (Bar Harbor, ME, USA). Blood was collected to measure the levels of serum aspartate aminotransferase, alanine aminotransferase, and blood urea nitrogen. All procedures complied with NIH guidelines and were approved by the Institutional Animal Care and Use Committee.

Primary Mouse Hepatocyte Isolation and Free Uptake Assay

Primary mouse hepatocytes were isolated from male BALB/c mice as described previously,⁴² and they were run over a Percoll gradient to

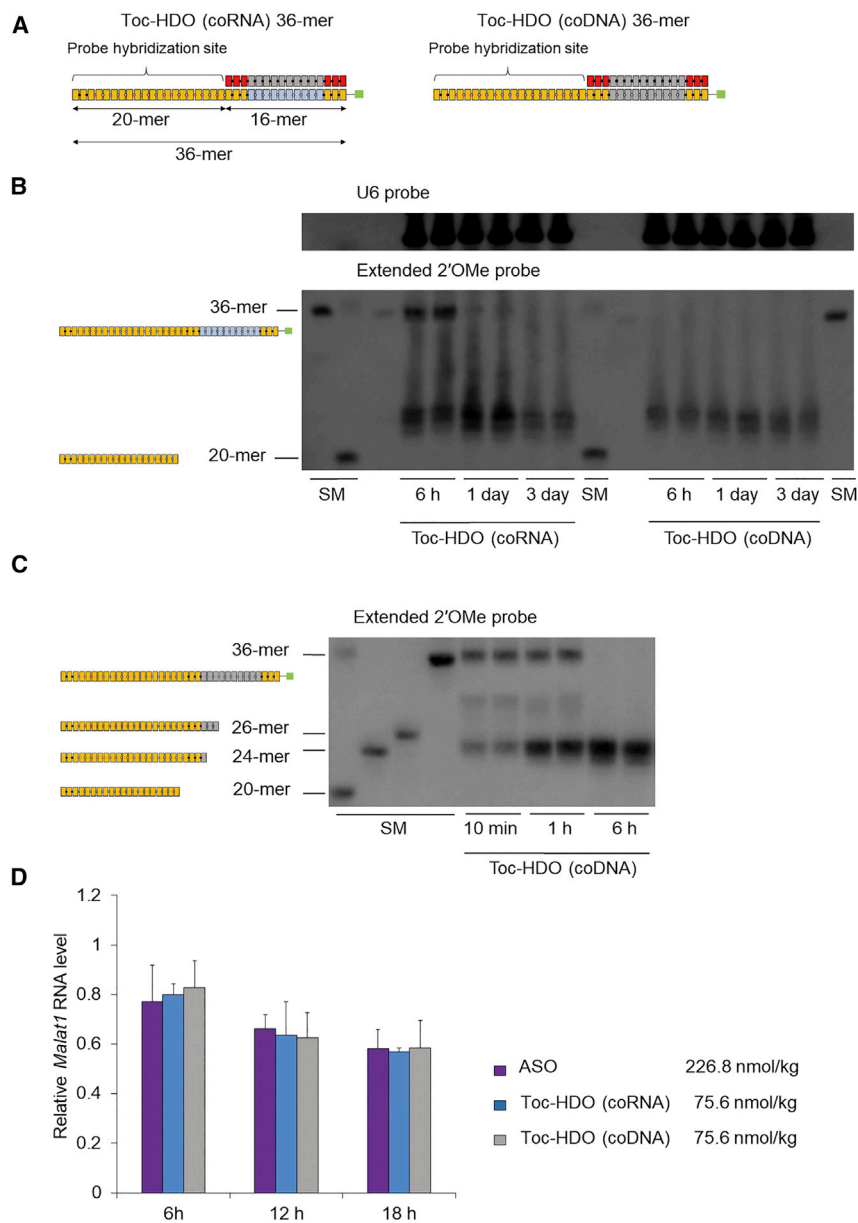


Figure 5. Cleavage of Toc-HDO (coRNA) and Toc-HDO (coDNA) Complementary Strands Using 16-mer *Malat1* Targeting ASO

(A) Structures of 16-mer *Malat1* targeting ASO/36-mer Toc-HDO (coRNA) and Toc-HDO (coDNA) with overhanging 20-mer PO 2'OMe and two PS linkages on the 3' end of the complementary strand. (B) Northern blot analysis using a probe for the overhanging portion of the 36-mer complementary strand. Oligonucleotides were extracted from mouse liver tissue at 6 h, 1 day, or 3 days after injection with the 36-mer Toc-HDO (coRNA) or Toc-HDO (coDNA) at a dose of 1,134 nmol/kg as the parent ASO. Size marker (SM) structures are illustrated on the left. (C) Northern blot analysis of mouse liver extracts at 10 min or 1 h after an injection of the 36-mer Toc-HDO (coDNA) at a dose of 1,134 nmol/kg. (D) Quantitative real-time PCR analysis of relative *Malat1* RNA expression levels in mouse liver 6, 12, and 18 h after the animals received intravenous injection of the parent ASO at a dose of 226.8 nmol/kg, or Toc-HDO (coRNA) or Toc-HDO (coDNA) at a dose of 75.6 nmol/kg.

cent nucleic acid stain that has maximum excitation/emission at 500 nm/525 nm when bound to RNA.

To detect DNA/LNA gapmers in mouse liver tissue, quantitative real-time PCR analysis was performed using a TaqMan microRNA reverse transcription kit (Applied Biosystems, Foster City, CA, USA) and a LightCycler 480 real-time PCR instrument (Roche Diagnostics, Basel, Switzerland), with data normalized to the mouse *U6* snRNA level. The primers and probes for DNA/LNA gapmers targeting mouse *Malat1* and *Apob* genes and mouse *U6* were designed by Applied Biosystems.

Northern Blot Analysis

Northern blot analysis of the Toc-HDO with the 36-mer coRNA/coDNA was performed as previously reported with slight modifications.¹³ Briefly, total RNA was extracted from mouse

Diagnosics, Basel, Switzerland). *Apob* mRNA and *Malat1* RNA levels were normalized to those of *Actb* mRNA. All of the experiments were performed in accordance with the Minimum Information for Publication of Quantitative Real-Time PCR Experiments (MIQE) guidelines.

The sequences of the primer and probe sets for mouse *Scarb1* were as follows: forward, 5'-TGACAACGACACCGTGTCT-3', reverse, 5'-ATGCGACTTGTGAGGCTGG-3', probe, 5'-CGTGGAGAACCGCAGCCTCCATT-3'. The levels of *Scarb1* mRNA transcripts were normalized to total RNA levels using RiboGreen RNA quantitation reagent (Molecular Probes). RiboGreen is an ultrasensitive fluores-

liver using Isogen II (Nippon Gene, Tokyo, Japan). Thirty micrograms of total RNA was separated by electrophoresis in an 18% polyacrylamide-7 M urea gel and transferred to a Hybond-N+ membrane (Amersham Biosciences, Piscataway, NJ, USA). The blot was hybridized with a probe corresponding to the sequence of the extended portion in coRNA/coDNA, or with a probe to *U6* snRNA as a loading control. Both probes were labeled with digoxigenin (DIG)-2',3'-deoxyuridine-5'-triphosphate (ddUTP) using a DIG oligonucleotide 3' end labeling kit, second generation (Roche Diagnostics, Basel, Switzerland). The sequence of the DNA probe for detecting extended 2'OMe was 5'-TGGTGGTGCATGCGTAGC-3'. The signals were visualized using a Gene Images CDP-Star detection kit (Amersham

Biosciences, Piscataway, NJ, USA), and band intensities were analyzed using Image Lab software version 5.2 of ChemiDoc Touch (Bio-Rad, Hercules, CA, USA).

Fluorescence-Based Determination of ASO Concentrations in the Liver

Liver samples were obtained from the mice i.v. injected with Cy5-labeled ASOs. Tissues were homogenized in 250 μ L of PBS (Nakarai, Kyoto, Japan), and Cy5 concentrations were measured using an i-control instrument (Tecan, Männedorf, Switzerland).

Statistical Analysis

Animal experiments were performed with three to four mice per treatment group. Pairwise comparisons were performed using the Student's *t* test. Multiple comparisons were performed using one-way analysis of variance (ANOVA) with post hoc Bonferroni's correction for multiple comparisons. Differences were considered significant when $p < 0.05$. All statistical analyses were performed using Prism version 6.05 (GraphPad, San Diego, CA, USA).

SUPPLEMENTAL INFORMATION

Supplemental Information can be found online at <https://doi.org/10.1016/j.ymthe.2020.10.017>.

ACKNOWLEDGMENTS

We thank Drs. Fumika Sakaue and Ken Asada (Department of Neurology and Neurological Science, Graduate School, Tokyo Medical and Dental University) for their technical support. This study was supported by grants from Core Research for Evolutional Science and Technology (CREST, JPMJCR12L4) and the Japan Science and Technology Agency, Japan to T.Y. This research was also supported by the Basic Science and Platform Technology Programs for Innovative Biological Medicine (18am0301003h0005) and Advanced Biological Medicine (20am0401006h0002) to T.Y., from the Japan Agency for Medical Research and Development (AMED; Tokyo, Japan), and a JSPS KAKENHI Grant-in-Aid for Scientific Research (S) (17H06109 to T.Y. and T.N.) and (B) (16H05221 to T.N.) from the Ministry of Education, Culture, Sports, Science, and Technology of Japan (MEXT) (Tokyo).

AUTHOR CONTRIBUTIONS

Y.A., T.N., K.Y., and T.Y. conceived the concept of Toc-HDO (coDNA); Y.A., T.N., C.F.B., P.P.S., and K.Y. designed the study; Y.A., T.K., and K.Y.-T. performed the experiments; Y.A., T.N., K.Y., P.P.S., and T.Y. wrote the manuscript.

DECLARATION OF INTERESTS

T.Y. collaborates with Daiichi Sankyo Company, Ltd; Mitsubishi Tanabe Pharma Corporation; Ono Pharmaceutical Company, Ltd; Rena Therapeutics, Inc.; Takeda Pharmaceutical Company, Ltd; Nanocarrier Pharmaceutical Company, Ltd; and Toray Industries, Inc., and serves as an academic adviser for Rena Therapeutics, Inc. The remaining authors declare no competing interests.

REFERENCES

- Bennett, C.F., Baker, B.F., Pham, N., Swayze, E., and Geary, R.S. (2017). Pharmacology of antisense drugs. *Annu. Rev. Pharmacol. Toxicol.* 57, 81–105.
- Seth, P.P., and Swayze, E.E. (2019). The medicinal chemistry of RNase H-activating antisense oligonucleotides. In *Advances in Nucleic Acid Therapeutics*, S. Agrawal and M.J. Gait, eds. (The Royal Society of Chemistry), pp. 32–61.
- Cerritelli, S.M., and Crouch, R.J. (2009). Ribonuclease H: the enzymes in eukaryotes. *FEBS J.* 276, 1494–1505.
- Lima, W., Wu, H., and Crooke, S.T. (2008). The RNase H mechanism. In *Antisense Drug Technology: Principles, Strategies, and Applications*, Second Edition, S.T. Crooke (CRC Press), pp. 47–74.
- Crooke, S.T., and Geary, R.S. (2013). Clinical pharmacological properties of mipomersen (Kynamro), a second generation antisense inhibitor of apolipoprotein B. *Br. J. Clin. Pharmacol.* 76, 269–276.
- Mendell, J.R., Rodino-Klapac, L.R., Sahenk, Z., Roush, K., Bird, L., Lowes, L.P., Alfano, L., Gomez, A.M., Lewis, S., Kota, J., et al.; Eteplirsen Study Group (2013). Eteplirsen for the treatment of Duchenne muscular dystrophy. *Ann. Neurol.* 74, 637–647.
- Hua, Y., Sahashi, K., Hung, G., Rigo, F., Passini, M.A., Bennett, C.F., and Krainer, A.R. (2010). Antisense correction of SMN2 splicing in the CNS rescues necrosis in a type III SMA mouse model. *Genes Dev.* 24, 1634–1644.
- Finkel, R.S., Mercuri, E., Darras, B.T., Connolly, A.M., Kuntz, N.L., Kirschner, J., Chiriboga, C.A., Saito, K., Servais, L., Tizzano, E., et al.; ENDEAR Study Group (2017). Nusinersen versus sham control in infantile-onset spinal muscular atrophy. *N. Engl. J. Med.* 377, 1723–1732.
- Mercuri, E., Darras, B.T., Chiriboga, C.A., Day, J.W., Campbell, C., Connolly, A.M., Iannaccone, S.T., Kirschner, J., Kuntz, N.L., Saito, K., et al.; CHERISH Study Group (2018). Nusinersen versus sham control in later-onset spinal muscular atrophy. *N. Engl. J. Med.* 378, 625–635.
- Gales, L. (2019). Tegsedi (inotersen): an antisense oligonucleotide approved for the treatment of adult patients with hereditary transthyretin amyloidosis. *Pharmaceuticals (Basel)* 12, 78.
- Gertz, M.A., Mauermann, M.L., Grogan, M., and Coelho, T. (2019). Advances in the treatment of hereditary transthyretin amyloidosis: a review. *Brain Behav.* 9, e01371.
- Crooke, S.T., Witztum, J.L., Bennett, C.F., and Baker, B.F. (2018). RNA-targeted therapeutics. *Cell Metab.* 27, 714–739.
- Nishina, K., Piao, W., Yoshida-Tanaka, K., Sujino, Y., Nishina, T., Yamamoto, T., Nitta, K., Yoshioka, K., Kuwahara, H., Yasuhara, H., et al. (2015). DNA/RNA heteroduplex oligonucleotide for highly efficient gene silencing. *Nat. Commun.* 6, 7969.
- Asami, Y., Yoshioka, K., Nishina, K., Nagata, T., and Yokota, T. (2016). Drug delivery system of therapeutic oligonucleotides. *Drug Discov. Ther.* 10, 256–262.
- Hara, R.I., Hisada, Y., Maeda, Y., Yokota, T., and Wada, T. (2018). Artificial cationic oligosaccharides for heteroduplex oligonucleotide-type drugs. *Sci. Rep.* 8, 4323.
- Kuwahara, H., Song, J., Shimoura, T., Yoshida-Tanaka, K., Mizuno, T., Mochizuki, T., Zeniya, S., Li, F., Nishina, K., Nagata, T., et al. (2018). Modulation of blood-brain barrier function by a heteroduplex oligonucleotide in vivo. *Sci. Rep.* 8, 4377.
- Yoshioka, K., Kunieda, T., Asami, Y., Guo, H., Miyata, H., Yoshida-Tanaka, K., Sujino, Y., Piao, W., Kuwahara, H., Nishina, K., et al. (2019). Highly efficient silencing of microRNA by heteroduplex oligonucleotides. *Nucleic Acids Res.* 47, 7321–7332.
- Keyel, P.A. (2017). Dnases in health and disease. *Dev. Biol.* 429, 1–11.
- Koizumi, T. (1995). Tissue distribution of deoxyribonuclease I (DNase I) activity level in mice and its sexual dimorphism. *Exp. Anim.* 44, 181–185.
- Evans, C.J., and Aguilera, R.J. (2003). DNase II: genes, enzymes and function. *Gene* 322, 1–15.
- Inoue, H., Hayase, Y., Imura, A., Iwai, S., Miura, K., and Ohtsuka, E. (1987). Synthesis and hybridization studies on two complementary nona(2'-O-methyl)ribonucleotides. *Nucleic Acids Res.* 15, 6131–6148.
- Sproat, B.S., Lamond, A.I., Beijer, B., Neuner, P., and Ryder, U. (1989). Highly efficient chemical synthesis of 2'-O-methyloligoribonucleotides and tetrabiotinylated derivatives; novel probes that are resistant to degradation by RNA or DNA specific nucleases. *Nucleic Acids Res.* 17, 3373–3386.

23. Campbell, J.M., Bacon, T.A., and Wickstrom, E. (1990). Oligodeoxynucleoside phosphorothioate stability in subcellular extracts, culture media, sera and cerebrospinal fluid. *J. Biochem. Biophys. Methods* *20*, 259–267.
24. Nishina, T., Numata, J., Nishina, K., Yoshida-Tanaka, K., Nitta, K., Piao, W., Iwata, R., Ito, S., Kuwahara, H., Wada, T., et al. (2015). Chimeric antisense oligonucleotide conjugated to α -tocopherol. *Mol. Ther. Nucleic Acids* *4*, e220.
25. Seth, P.P., Siwkowski, A., Allerson, C.R., Vasquez, G., Lee, S., Prakash, T.P., Wancewicz, E.V., Witchell, D., and Swayze, E.E. (2009). Short antisense oligonucleotides with novel 2'-4' conformationally restricted nucleoside analogues show improved potency without increased toxicity in animals. *J. Med. Chem.* *52*, 10–13.
26. Murray, S., Ittig, D., Koller, E., Berdeja, A., Chappell, A., Prakash, T.P., Norrbom, M., Swayze, E.E., Leumann, C.J., and Seth, P.P. (2012). TricycloDNA-modified oligo-2'-deoxyribonucleotides reduce scavenger receptor B1 mRNA in hepatic and extra-hepatic tissues—a comparative study of oligonucleotide length, design and chemistry. *Nucleic Acids Res.* *40*, 6135–6143.
27. Croke, S.T., Wang, S., Vickers, T.A., Shen, W., and Liang, X.H. (2017). Cellular uptake and trafficking of antisense oligonucleotides. *Nat. Biotechnol.* *35*, 230–237.
28. Shemesh, C.S., Yu, R.Z., Gaus, H.J., Seth, P.P., Swayze, E.E., Bennett, F.C., Geary, R.S., Henry, S.P., and Wang, Y. (2016). Pharmacokinetic and pharmacodynamic investigations of ION-353382, a model antisense oligonucleotide: using alpha-2-macroglobulin and murinoglobulin double-knockout mice. *Nucleic Acid Ther.* *26*, 223–235.
29. Miller, C.M., Donner, A.J., Blank, E.E., Egger, A.W., Kellar, B.M., Østergaard, M.E., Seth, P.P., and Harris, E.N. (2016). Stabilin-1 and Stabilin-2 are specific receptors for the cellular internalization of phosphorothioate-modified antisense oligonucleotides (ASOs) in the liver. *Nucleic Acids Res.* *44*, 2782–2794.
30. Kzhyshkowska, J., Gratchev, A., and Goerdts, S. (2006). Stabilin-1, a homeostatic scavenger receptor with multiple functions. *J. Cell. Mol. Med.* *10*, 635–649.
31. Deshpande, D., Toledo-Velasquez, D., Thakkar, D., Liang, W., and Rojanasakul, Y. (1996). Enhanced cellular uptake of oligonucleotides by EGF receptor-mediated endocytosis in A549 cells. *Pharm. Res.* *13*, 57–61.
32. Wang, S., Allen, N., Vickers, T.A., Revenko, A.S., Sun, H., Liang, X.H., and Croke, S.T. (2018). Cellular uptake mediated by epidermal growth factor receptor facilitates the intracellular activity of phosphorothioate-modified antisense oligonucleotides. *Nucleic Acids Res.* *46*, 3579–3594.
33. Prakash, T.P., Graham, M.J., Yu, J., Carty, R., Low, A., Chappell, A., Schmidt, K., Zhao, C., Aghajan, M., Murray, H.F., et al. (2014). Targeted delivery of antisense oligonucleotides to hepatocytes using triantennary *N*-acetyl galactosamine improves potency 10-fold in mice. *Nucleic Acids Res.* *42*, 8796–8807.
34. Gaus, H.J., Gupta, R., Chappell, A.E., Østergaard, M.E., Swayze, E.E., and Seth, P.P. (2019). Characterization of the interactions of chemically-modified therapeutic nucleic acids with plasma proteins using a fluorescence polarization assay. *Nucleic Acids Res.* *47*, 1110–1122.
35. Majer, O., Liu, B., and Barton, G.M. (2017). Nucleic acid-sensing TLRs: trafficking and regulation. *Curr. Opin. Immunol.* *44*, 26–33.
36. Prakash, V., Tsekouras, K., Venkatachalapathy, M., Heinicke, L., Pressé, S., Walter, N.G., and Krishnan, Y. (2019). Quantitative mapping of endosomal DNA processing by single molecule counting. *Angew. Chem. Int. Ed. Engl.* *58*, 3073–3076.
37. Kailasan Vanaja, S., Rathinam, V.A., Atianand, M.K., Kalantari, P., Skehan, B., Fitzgerald, K.A., and Leong, J.M. (2014). Bacterial RNA:DNA hybrids are activators of the NLRP3 inflammasome. *Proc. Natl. Acad. Sci. USA* *111*, 7765–7770.
38. Kawasaki, A.M., Casper, M.D., Freier, S.M., Lesnik, E.A., Zounes, M.C., Cummins, L.L., Gonzalez, C., and Cook, P.D. (1993). Uniformly modified 2'-deoxy-2'-fluoro phosphorothioate oligonucleotides as nuclease-resistant antisense compounds with high affinity and specificity for RNA targets. *J. Med. Chem.* *36*, 831–841.
39. Shen, W., De Hoyos, C.L., Sun, H., Vickers, T.A., Liang, X.H., and Croke, S.T. (2018). Acute hepatotoxicity of 2' fluoro-modified 5-10-5 gapmer phosphorothioate oligonucleotides in mice correlates with intracellular protein binding and the loss of DBHS proteins. *Nucleic Acids Res.* *46*, 2204–2217.
40. Tanji, H., Ohto, U., Shibata, T., Taoka, M., Yamauchi, Y., Isobe, T., Miyake, K., and Shimizu, T. (2015). Toll-like receptor 8 senses degradation products of single-stranded RNA. *Nat. Struct. Mol. Biol.* *22*, 109–115.
41. Desmet, C.J., and Ishii, K.J. (2012). Nucleic acid sensing at the interface between innate and adaptive immunity in vaccination. *Nat. Rev. Immunol.* *12*, 479–491.
42. Tanowitz, M., Hettrick, L., Revenko, A., Kinberger, G.A., Prakash, T.P., and Seth, P.P. (2017). Asialoglycoprotein receptor 1 mediates productive uptake of *N*-acetylgalactosamine-conjugated and unconjugated phosphorothioate antisense oligonucleotides into liver hepatocytes. *Nucleic Acids Res.* *45*, 12388–12400.
43. Severgnini, M., Sherman, J., Sehgal, A., Jayaprakash, N.K., Aubin, J., Wang, G., Zhang, L., Peng, C.G., Yucius, K., Butler, J., and Fitzgerald, K. (2012). A rapid two-step method for isolation of functional primary mouse hepatocytes: cell characterization and asialoglycoprotein receptor based assay development. *Cytotechnology* *64*, 187–195.